ISSN: 2455 - 1597

ijergs
Open Access

International Journal of Engineering Research and Generic Science (IJERGS)
Available online at: https://www.ijergs.in

Volume - 5, Issue - 6, November – December - 2019, Page No. 19 - 26

Review paper on Analysis of CNN approach for Lung Cancer Detection and Classification

[1]Dr. Sheetanshu Rajoriya, Supervisior, Sunrise University, Alwar

[2]Pramod Kumar Sharma, Scholar, Sunrise University, Alwar

Abstract

This paper shows a computer-aided diagnostic (CAD) method, a dataset from the for lung cancer classification of CT scans with unmarked nodules. As an initial segmentation approach, thresholding was used to segment out lung tissue from the remainder of the CT scan. The next finest lung segmentation was created by Thresholding. The initial solution was to feed the segmented CT scans directly for classification into 3D CNNs, but this proved to be insufficient. Instead, the first identification of nodule candidates in the CT scans was performed by an updated U-Net trained on LUNA16 data (CT scans with labelled nodules). In order to identify the CT scan as positive or negative for lung cancer, the U-Net nodule detection provided several false positives, so regions of CTs with segmented lungs where the most likely nodule candidates were located as defined by the U-Net production were fed into 3D Convolutional Neural Networks (CNNs). The 3D CNNs provided the Accuracy O Test Set. Our CAD system's efficiency outperforms the existing literature CAD systems that have many preparation and testing levels, each involving a lot of labelled data, whereas our CAD system has only three key stages (segmentation, nodule candidate identification, and classification of malignancy), allowing more effective training and detection and more generalization for other cancers

Keywords: Lung cancer; computed tomography; deep learning; Convolutional neural networks; segmentation

Introduction

Lung cancer is one of the most prevalent diseases responsible for over 225,000 cases, 150,000 deaths, and $12 billion in total health care expenses. It is also one of the worst cancers; nationally, only 17 percent of people diagnosed with lung cancer in the country live five years after diagnosis, although in developed countries, the mortality rate is smaller. A cancer's level corresponds to how deeply it has metastasized. Stages 1 and 2 refer to cancers found in the lungs, and cancers that have spread to other organs refer to the later stages. Present screening procedures, such as CT scans, include biopsies and imaging. Early diagnosis of lung cancer (detection during the earlier stages) greatly increases the probability of survival, but early detection of lung cancer is often more difficult when less symptoms are present. [1].

In patient CT scans of lungs with and without early stage lung cancer, our job is a binary classification question to diagnose the existence of lung cancer. To create an accurate classifier, we aim to use techniques from computer vision and deep learning, particularly 2D and 3D convolutionary neural networks. An correct classification of lung cancer could accelerate and reduce the cost of screening for lung cancer, encouraging more universal screening.

Early identification and survival change. The aim is to build a computer-aided diagnostic (CAD) system that involves patient chest CT scans and outputs as an input, whether the patient has lung cancer or not. [2].

Although this job sounds simple, in the haystack dilemma it is really a needle. The CAD device will have to detect the presence of a small nodule (< 10 mm in diameter for early stage cancers) from a large 3D lung CT scan to determine whether or not a patient has early-stage cancer (typically around 200 mm 400 mm 400 mm). An example of an early stage

nodule of lung cancer seen in a 2D slice of a CT scan is given in Fig. 1. In addition, a CT scan is packed with noise from nearby tissues, bone, air, so this noise will first have to be preprocessed for the CAD systems search to be successful. Therefore, image preprocessing, nodule candidate identification, malignancy classification are our classification pipeline.

In this article, we use systematic preprocessing procedures to extract specific nodules in order to increase the precision of lung cancer diagnosis. In addition, we conduct CNN end-to-end testing from scratch in order to understand the full capacity of the neural network, i.e. to acquire discriminatory characteristics. A dataset containing lung nodules from more than 1390 low dose CT scans is used for detailed experimental assessments.

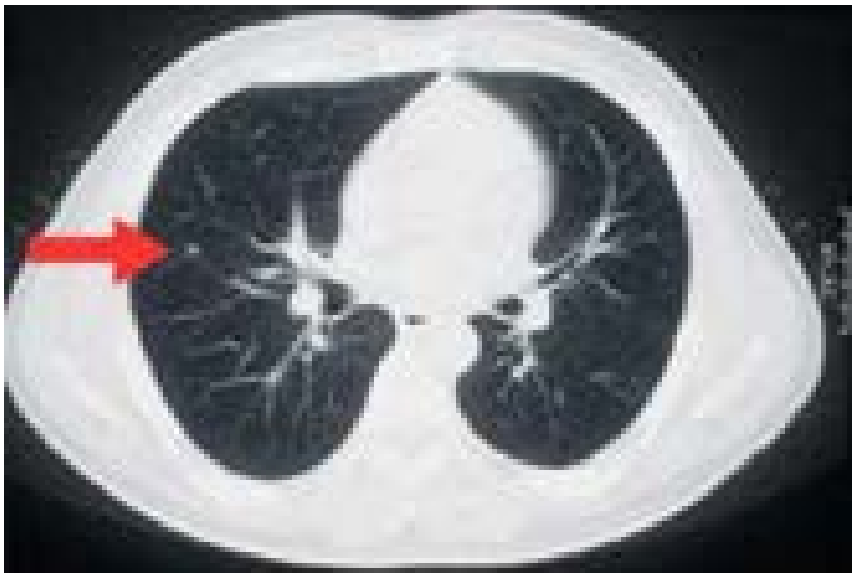

Figure 1: 2D CT scan slice containing a small (5mm) early stage lung cancer nodule.

Related Work

Recently, deep artificial neural networks have been applied in many applications in pattern recognition and machine learning, especially, Convolutional neural networks (CNNs) which is one class of models [3]. Another approach of CNNs was applied on ImageNet Classification in 2012 is called an ensemble CNNs which outperformed the best results which were popular in the computer vision community [4]. There has also been popular latest research in the area of medical imaging using deep learning with promising results.

R. Golan proposed a framework that trains the weights of the CNN by a back propagation to detect lung nodules in the CT image sub-volumes. This system achieved sensitivity of 78.9% with 20 false positives, while 71.2% with 10 FPs per scan, on lung nodules that have been annotated by all four radiologists.

Convolutional neural networks have achieved better than Deep Belief Networks in current studies on benchmark computer vision datasets. The CNNs have attracted considerable interest in machine learning since they have strong representation ability in learning useful features from input data in recent years.

Data

Our primary dataset is the patient lung CT scan dataset from Cancer Hospital. The dataset contains labeled data for 1475 patients, which we divide into training set of size 900, and test set of size 575. For each patient, the data consists of CT scan data and a label (0 for no cancer, 1 for cancer). Note that the dataset does not have labeled nodules. For each

patient, the CT scan data consists of a variable number of images (typically around 100- 400, each image is an axial slice) of 512 512 pixels. The slices are provided in DICOM format. Around 70% of the provided labels in the dataset are 0, so we used a weighted loss function in our malignancy classifier to address this imbalance.

Dataset alone proved to be inadequate to accurately classify the validation set, we also used the patient lung CT scan dataset with labeled nodules from the Lung Nodule Analysis 2016 (LUNA16) Challenge to train a U-Net for lung nodule detection. The LUNA16 dataset contains labeled data for 888 patients, which we divided into a training set of size 710 and a validation set of size 178. For each patient, the data consists of CT scan data and a nodule label (list of nodule center coordinates and diameter). For each patient, the CT scan data consists of a variable number of images (typically around 100-400, each image is an axial slice) of 512 × 512 pixels. LUNA16 data was used to train a U-Net for nodule detection, one of the phases in our classification pipeline. The problem is to accurately predict a patient's label ('cancer' or 'no cancer') based on the patient's Kaggle lung CT scan. We will use accuracy, sensitivity, specificity, and AUC of the ROC to evaluate our CAD system's performance on the test set.

Methods

Typical CAD systems for lung cancer have the following pipeline: image preprocessing, detection of cancerous nodule candidates, nodule candidate false positive reduction, malig- nancy prediction for each nodule candidate, and malignancy prediction for overall CT scan [15]. These pipelines have many phases, each of which are computationally expensive and require well-labeled data during training. For example, the false positive reduction phase requires a dataset of labeled true and false nodule candidates, and the nodule malignancy prediction phase requires a dataset with nodules labeled with malignancy.

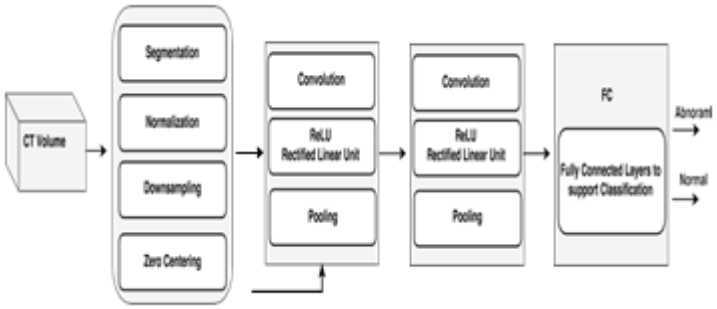

Figure 2: 3D Convolutional neural networks architecture

True/False labels for nodule candidates and malignancy labels for nodules are sparse for lung cancer, and may be nonexistent for some other cancers, so CAD systems that rely on such data would not generalize to other cancers. In order to achieve greater computational efficiency and generalizability to other cancers, the proposed CAD system has shorter pipeline and only requires the following data during training: a dataset of CT scans with true nodules labeled, and a dataset of CT scans with an overall malignancy label. State-of-the-art CAD systems that predict malignancy from CT scans achieve AUC of up to 0.83 [16]. However, as mentioned above, these systems take as input various labeled data that is not used in this framework. The main goal of the proposed system is to reach close to this performance.

The proposed CAD system starts with preprocessing the 3D CT scans using segmentation, normalization, down sampling, and zero-centering. The initial approach was to simply input the preprocessed 3D CT scans into 3D CNNs, but the results

were poor. So an additional preprocessing was performed to input only regions of interests into the 3D CNNs. To identify regions of interest, a U-Net was trained for nodule candidate detection. Then input regions around nodule candidates detected by the U-Net was fed into 3D CNNs to ultimately classify the CT scans as positive or negative for lung cancer. The overall architecture is shown in Fig. 2, all details of layers will be described in the next sections.

A. Preprocessing and Segmentation

For each patient, pixel values was first converted in each image to Hounsfield units (HU), a measurement of radio density, and 2D slices are stacked into a single 3D image. Because tumors form on lung tissue, segmentation is used to mask out the bone, outside air, and other substances that would make data noisy, and leave only lung tissue information for the classifier. A number of segmentation approaches were tried, including thresholding, clustering (Kmeans and Meanshift), and Watershed. K-means and Meanshift allow very little super- vision and did not produce good qualitative results. Watershed produced the best qualitative results, but took too long to run to use by the deadline. Ultimately, thresholding was used.

After segmentation, the 3D image is normalized by applying the linear scaling to squeeze all pixels of the original un segmented image to values between 0 and 1. Spline interpolation down samples each 3D image by a scale of 0.5 in each of the three dimensions. Finally, zero-centering is performed on data by subtracting the mean of all the images from the training set.

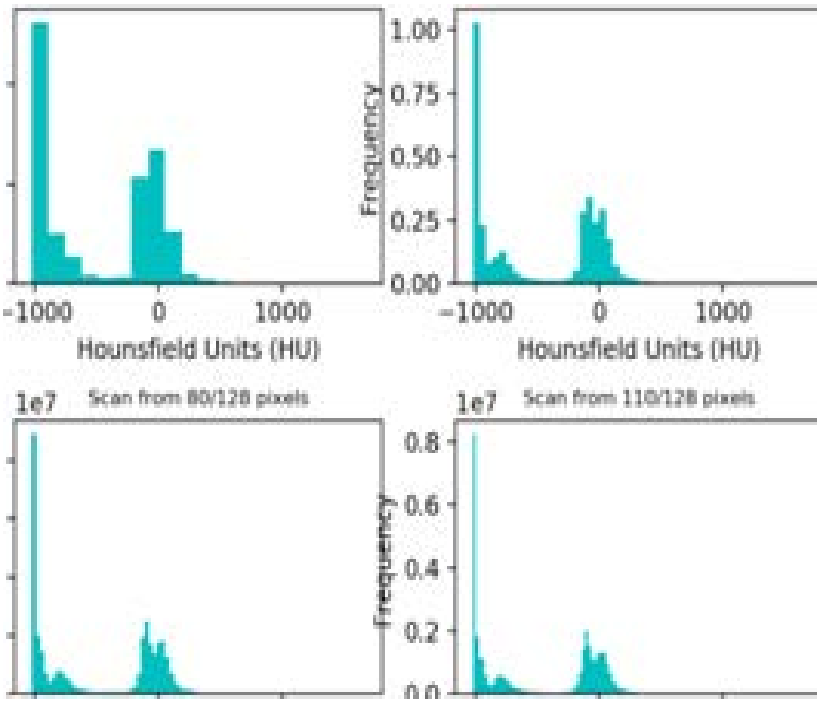

(a).Histograms of pixel values in HU for sample patients CT scan at various slices.

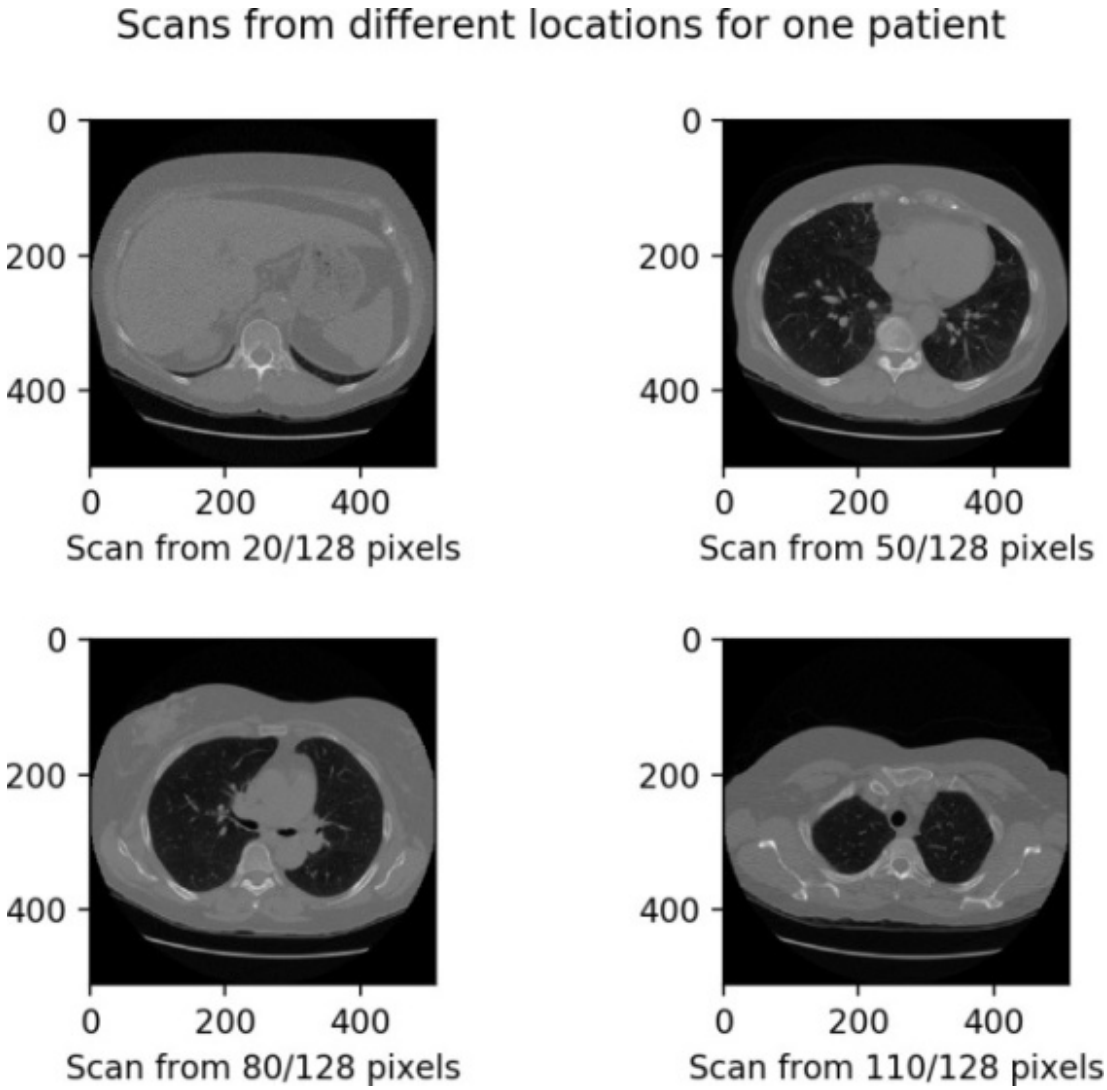

(b). Ccorresponding 2D axial slices.

Figure 3: Histogram of HU values at 3b corresponding axial slices for sample patient 3D image at various axial.

Simulation Results

The experiments are conducted using DSB dataset. In this dataset, a thousand low-dose CT images from high-risk patients in DICOM format is given. The DSB database consists of 1397 CT scans and 248580 slices. Each scan contains a series with multiple axial slices of the chest cavity. Each scan has a variable number of 2D slices (Fig. 4), which can vary based on the machine taking the scan and patient. The DICOM files have a header that contains the necessary information about the patient id, as well as scan parameters such as the slice thickness. It is publicly available in the . Dicom is the de-facto file standard in medical imaging. This pixel size/coarseness of the scan differs from scan to scan (e.g. the distance between slices may differ), which can hurt performance of our model.

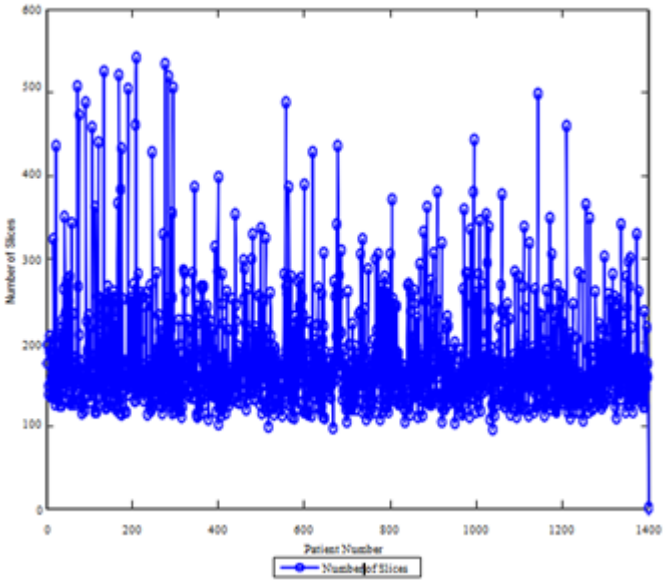

Figure 4: Number of slices per patient in data science bowl dataset.

The accuracy metric is the used metric in our evaluations. In our first set of experiments we considered a range of CNN architectures for the binary classification task. Early experi- mentation suggested that the number of filters and neurons per layer were less significant than the number of layers. Thus, to simplify analysis the first Convolutional layer used seven filters with size 5 5 5, the second Convolutional layer used 17 filters with 5 5 3 and all fully connected layers used 256 neurons. These were found to generally perform well and we considered the impact of one or two Convolutional layers followed by one or two fully connected layers. The networks were trained as described above and the results of these experiments can be found in Table I. Our results suggest that two Convolutional layers followed by a single hidden layer is one of the optimal network architecture for this dataset. The average error for training .

Another important parameter in the training of neural networks is the number of observations that are sampled at each iteration, the size of the so-called mini batch.

The use of mini batches is often driven in part by computational considerations but can impact the ability of SGD to find a good solution. Indeed, we found that choosing the proper mini batch size was critical for learning to be effective. We tried mini batches of size 1, 10, 50 and 100. While the nature of SGD suggests that larger batch sizes should produce better gradient estimates and there for work better, our results here show that the opposite is true. Smaller batch sizes, even as small as 1, produce the best results. We suspect that the added noise of smaller batch sizes allows SGD to better escape poor local optima and thus perform better overall.

The recognition results are shown by confusion matrix achieved on the DSB dataset with 3D CNN as shown in Table

As shown from the Table, Accuracy of model is 86.6%, Misclassification rate is 13.4%, False positive rate is 11.9%, and False Negative is 14.7%. Almost all patients are classified correctly. Additionally, there is an enhancement on accuracy due to efficient U-Net architecture and segmentation.

Actual	Abnormal	Normal
Abnormal	**0.853**	0.147
Normal	0.119	**0.881**

Table I: Confusion Matrix of 3D CNN using 30% Testing

Conclusion

In this paper, discussed a deep Convolutional neural network (CNN) architecture to detect nodules in patients of lung cancer and detect the interest points using U-Net architecture. This step is a preprocessing step for 3D CNN. The deep 3D CNN models performed the best on the test set. While we achieve state-of-the-art performance AUC of 0.83, we perform well considering that we use less labeled data than most state- of-the-art CAD systems. As an interesting observation, The first layer is a preprocessing layer for segmentation using different techniques. Threshold, Watershed, and U-Net are used to identify the nodules of patients.

The network can be trained end-to-end from raw image patches. Its main requirement is the availability of training database, but otherwise no assumptions are made about the objects of interest or underlying image modality.

In the future, it could be possible to extend our current model to not only determine whether or not the patient has cancer, but also determine the exact location of the cancerous nodules. The most immediate future work is to use Watershed segmentation as the initial lung segmentation. Other opportunities for improvement include making the network deeper, and more extensive hyper parameter tuning. Also, we saved our model parameters at best accuracy, but perhaps we could have saved at other metrics, such as F1. Other future work include extending our models to 3D images for other cancers. The advantage of not requiring too much labeled data specific to our cancer is it could make it generalizable to other cancers.

References

1. W.-J. Choi and T.-S. Choi, "Automated pulmonary nodule detection system in computed tomography images: A hierarchical block classifi- cation approach," *Entropy*, vol. 15, no. 2, pp. 507–523, 2013.
2. A. Chon, N. Balachandar, and P. Lu, "Deep Convolutional neural networks for lung cancer detection," tech. rep., Stanford University, 2017.
3. Y. LeCun, K. Kavukcuoglu, and C. Farabet, "Convolutional networks and applications in vision.," in *Proceedings of the IEEE International Symposium on Circuits and Systems (ISCAS)*, pp. 253–256, IEEE, 2010.
4. K. Alex, I. Sutskever, and G. E. Hinton, "Imagenet classification with deep convolutional neural networks," in *Advances in Neural Information Processing Systems 25 (NIPS 2012)* (F. Pereira, C. J. C. Burges, L. Bottou, and K. Q. Weinberger, eds.), pp. 1097–1105, 2012.
5. H. Suk, S. Lee, and D. Shen, "Hierarchical feature representation and multimodal fusion with deep learning for AD/MCI diagnosis," *NeuroImage*, vol. 101, pp. 569–582, 2014.
6. G. Wu, M. Kim, Q. Wang, Y. Gao, S. Liao, and D. Shen, "Unsupervised deep feature learning for deformable registration of mr brain images.," *Medical Image Computing and Computer-Assisted Intervention*, vol. 16, no. Pt 2, pp. 649–656, 2013.

7. Y. Xu, T. Mo, Q. Feng, P. Zhong, M. Lai, and E. I. Chang, "Deep learning of feature representation with multiple instance learning for medical image analysis," in *IEEE International Conference on Acoustics, Speech and Signal Processing, ICASSP*, pp. 1626–1630, 2014.
8. D. Kumar, A. Wong, and D. A. Clausi, "Lung nodule classification using deep features in ct images," in *2015 12th Conference on Computer and Robot Vision*, pp. 133–138, June 2015.
9. Y. Bar, I. Diamant, L. Wolf, S. Lieberman, E. Konen, and H. Greenspan, "Chest pathology detection using deep learning with non-medical train- ing," *Proceedings - International Symposium on Biomedical Imaging*, vol. 2015-July, pp. 294–297, 2015.
10. W. Sun, B. Zheng, and W. Qian, "Computer aided lung cancer diagnosis with deep learning algorithms," in *SPIE Medical Imaging*, vol. 9785, pp. 97850Z–97850Z, International Society for Optics and Photonics, 2016.
11. J. Tan, Y. Huo, Z. Liang, and L. Li, "A comparison study on the effect of false positive reduction in deep learning based detection for juxtapleural lung nodules: Cnn vs dnn," in *Proceedings of the Symposium on Modeling and Simulation in Medicine*, MSM '17, (San Diego, CA, USA), pp. 8:1–8:8, Society for Computer Simulation International, 2017.
12. R. Golan, C. Jacob, and J. Denzinger, "Lung nodule detection in ct im- ages using deep Convolutional neural networks," in *2016 International Joint Conference on Neural Networks (IJCNN)*, pp. 243–250, July 2016.
13. Kaggle, "Data science bowl 2017." https://www.kaggle.com/c/data- science-bowl-2017/data, 2017.
14. LUNA16, "Lung nodule analysis 2016." https://luna16.grand- challenge.org/, 2017.
15. M. Firmino, A. Morais, R. Mendoa, M. Dantas, H. Hekis, and R. Valentim, "Computer-aided detection system for lung cancer in computed tomography scans: Review and future prospects," *BioMedical Engineering OnLine*, vol. 13, p. 41, 2014.
16. S. Hawkins, H. Wang, Y. Liu, A. Garcia, O.Stringfield, H. Krewer,Q. Li, D. Cherezov, R. A. Gatenby, Y. Balagurunathan, D. Goldgof, M. B. Schabath, L. Hall, and R. J. Gillies, "Predicting malignant nodules from screening ct scans," *Journal of Thoracic Oncology*, vol. 11, no. 12, pp. 2120–2128, 2016.
17. M. S. AL-TARAWNEH, "Lung cancer detection using image processing techniques," *Leonardo Electronic Journal of Practices and Technolo- gies*, pp. 147–158, June 2012.
18. O. Ronneberger, P. Fischer, and T. Brox, "U-net: Convolutional net- works for biomedical image segmentation," *CoRR*, vol. abs/1505.04597, 2015.